frontiers in Energy Research

ORIGINAL RESEARCH
published: 04 February 2022
doi: 10.3389/fenrg.2022.828594

# Study of the Performance of a Thermoelectric Refrigeration Membrane Cold Chamber Distillation Component

*Junhu Hu*[1], *Shunli Wu*[2], *Hao Liu*[1] *and Xiaohong Yang*[1,3]*

[1]College of Energy and Power Engineering, Inner Mongolia University of Technology, Hohhot, China, [2]Institute of Advanced Interdisciplinary Materials Science, Shanghai University, Shanghai, China, [3]Inner Mongolia Key Laboratory for Renewable Energy, Hohhot, China

Thermoelectric Refrigeration Membrane Distillation (TERMD) is an emerging membrane-based evaporation technology with excellent prospects for separation industries. However, the development of the TERMD system was further limited by excellent membrane component properties. In this paper, a cold chamber component of a TERMD is manufactured. Then, the cooling performance of the component is studied to examine the coupling between the Thermoelectric Refrigeration (TER) and the Membrane Distillation (MD) process. Moreover, the effects of the membrane components properties are studied by changing the water flow rate, and the input current of thermoelectric refrigeration. The results showed that when the TERMD cold room inlet current is maintained stable and the heat dissipation intensity increases, the cooling temperature gradually decreases. Also, the temperature on the cold side tends to stabilize while the flow rate exceeds 600 L/h. In addition, the input power decreases as the heat dissipation intensity increases in the cooling dissipation intensity of the Thermoelectric Refrigeration Component (TERC) cold chamber is kept stable. And, the input power will reach a critical value while the water volume flow rate is over 500 L/h. Furthermore, the cooling rate reaches the maximum of 1.59 at the water volume flow rate of 700 L/h while the operating current of the TERC is 12 A. It is concluded that the thermoelectric refrigeration component can supply great refrigeration power and a high Coefficient of Performance (COP) under small current conditions for the analysis of the thermoelectric performance of the TERC.

**Keywords: thermoelectric refrigeration, heat dissipation, intensity threshold, membrane distillation, thermoelectric characteristics**

OPEN ACCESS

***Edited by:***
*Saleh Shalaby,*
*Tanta University, Egypt*

***Reviewed by:***
*Rubina Bahar,*
*Tunku Abdul Rahman University, Malaysia*
*A. E. Kabeel,*
*Tanta University, Egypt*

***Correspondence:**
*Xiaohong Yang*
*yxh1109@163.com*

***Specialty section:***
*This article was submitted to Solar Energy, a section of the journal Frontiers in Energy Research*

***Received:*** *03 December 2021*
***Accepted:*** *11 January 2022*
***Published:*** *04 February 2022*

***Citation:***
*Hu J, Wu S, Liu H and Yang X (2022) Study of the Performance of a Thermoelectric Refrigeration Membrane Cold Chamber Distillation Component. Front. Energy Res. 10:828594. doi: 10.3389/fenrg.2022.828594*

## INTRODUCTION

Water is the most plentiful resource of the earth. However, only 3% of the water is fresh and just about 0.5% of freshwater is accessible to human needs in river water or groundwater (Shtull-Trauring et al., 2020; Nthunya et al., 2022). Seawater desalination technologies are growing rapidly in coastal distinct where freshwater resources are scarce (Ma et al., 2021). Extraordinarily, Membrane distillation is a developing membrane separation technology through which combined membrane technique with distillation process (Liu et al., 1998; Meindersma et al., 2006; Liao

et al., 2021), which has been indicated that the membrane distillation possessed excellent advantages, e.g., high separation efficiency, simple operation conditions, mild requirements on the interaction between membrane, and raw feed liquid (Smolders and Franken, 1989; Rezaei et al., 2018). Therefore, it is widely applied to seawater desalination, ultra-pure water preparation, and separation of an azeotropic mixture the like (Gong et al., 2019; Karahan et al., 2020; DuChanois et al., 2021). However, refrigerating capacity required for the membrane distillation process is generally supplied by mechanical refrigeration, which causes a membrane distillation system to have a complex structure and higher power consumption. Fortunately, a novel refrigeration method has been presented. The TER is supported by the Peltier effect of the thermoelectric materials, which could directly transform electrical energy into temperature. (Alhuyi Nazari et al., 2021). TER as a solid-state cooling strategy has drawn extensive attention due to its compactness, reliability, small noise, environmental friendliness, cooling rapidness, and no mechanical moving parts cleanliness, easy to regulate and minimize (Pourkiaei et al., 2019). TER also applied to solar semiconductor refrigerators (Long et al., 2016a; Long et al., 2016b), semiconductor air-conditioned beds (Min et al., 2004; Wang et al., 2021), air conditioners, (Eslami et al., 2018), respectively. In addition, several considerable approaches have been reported to reveal the relation between the water distillation system and TERC (Rahbar et al., 2016; Al-Madhhachi and Min, 2017; Al-Nimr and Al-Ammari, 2020; Javadi Yanbolagh et al., 2020; Parsa et al., 2020). Traditionally, TER has been deployed directly for cooling in the distillation field, and the COP mainly relies on water vapor temperature (Al-Madhhachi et al., 2018). Importantly, the combined membrane distillation with TER is an emerging strategy in the water distillation field. Such as a self-contained direct contact membrane distillation (EPSCD) system which is integrated TERC and combined multistage MD a single unit to manage the energy requirement of the desalination process (Makanjuola et al., 2021). However, this system obtained high effectively by sacrificing simple structure. Furthermore, our group's previous investigation of the MD process and thermoelectric refrigerator (Junhu et al., 2015; Da et al., 2019), defined the coupling characteristic parameters, coupling conditions, optimal coupling conditions, and established the coupling characteristic parameter equation. Also, they found that the feed concentration, flow state, and membrane structure remain stable, the membrane distillation flux is controlled by the temperature difference on both sides of the membrane. Additionally, two criteria for determining the maximum water yield and optimal economy were proposed (Xh Yang and Li, 2015; Junhu et al., 2017). From the previous investigation, we designed a simple TERC to benefit TERMD in this work. In this study, a new TERMDC was designed, which the thermoelectric properties were investigated based on the existed experimental platform. To realize the application of the TERMD system, this paper mainly researched the performance and influencing factors of TERC and TERMDC under limited cooling conditions, for example, the influence of hot side heat dissipation intensity on refrigeration temperature and TERC input power. In addition, the operational stability of the thermoelectric refrigeration component was also analyzed to provide a reference for studying operation conditions of coupling between the TERC and the air gap MD process.

# MATERIALS AND METHODS

## Thermoelectric Refrigeration Air Gap Membrane Distillation System

Based on the solar air gap membrane distillation system, thermoelectric cooling technology is introduced to form a new-type solar TERMD system. As shown in **Figure 1**, firstly, raw feed liquid enters the cold chamber of the air gap membrane distillation system after preliminary water treatment in a pre-processing device. Next, it absorbs heat transferred from the hot end face of the thermoelectric refrigerator in the cold chamber and enters a heat exchanger after being preheated. Then, it absorbs heat supplied by a solar heat collection system and enters a hot chamber after working temperature has been reached. Furthermore, the high-temperature raw liquid in the hot chamber is vaporized in a gas-liquid boundary layer on a surface of the hot side of the membrane. The vaporized water vapor molecules diffuse to penetrate through membrane holes into the air gap. The water vapor molecules absorb the refrigeration capacity released by the thermoelectric refrigerator, the part of which is condensed into the water on the surface of the cold side of the membrane and in the air gap. The remaining part diffuses and coagulates into pure water on the cold wall. Lastly, the pure water condensed from the air gap is collected by a distilled water collection device. The concentrated high-temperature raw liquid is mixed with preheated raw liquid in the heat exchanger and energy supplied by the solar heat collection system.

The difference in temperature of the membrane two sides is the key factor in TERMDC. The hot side of TERMDC is attached to the cold chamber, the cold wall is attached to the cold side of the TER sheet, and the heating chamber is combined to form a novel structure of TERMDC. The refrigeration performance of the thermoelectric cooler is used to provide cooling capacity for the MD process. Meanwhile, the cold and heat temperature difference of the membrane is formed with the heating chamber. So that the steam pressure difference between the two sides of the membrane is generated, and the mass transfer driving force is provided for the membrane distillation process.

## Experimental Bench and System Procedure

To study the coupling between the thermoelectric refrigeration and the membrane distillation process, a TERMD cold chamber component is designed and then studied the performance.

The composition of the thermoelectric refrigeration experiment system is shown in **Figure 2A**. Circulating cooling water in a water tank is pressurized by a magnetic circulating pump and then input to the TERMDC cold chamber. In addition, the circulating cooling water performs heat exchange by an insertion-type heat radiator and then returns to the water storage tank.

The voltage and current stabilization power supply direct current to the thermoelectric refrigerator by a distribution box

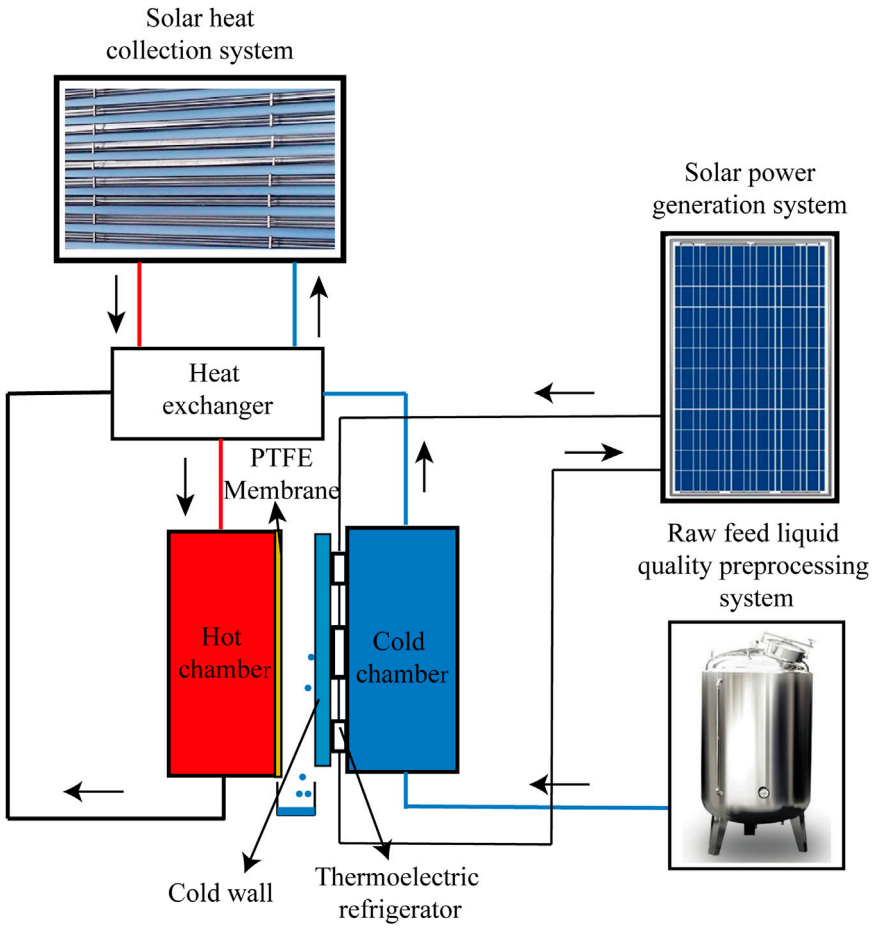


**FIGURE 1 |** Schematic of a thermoelectric refrigeration air gap membrane distillation system.

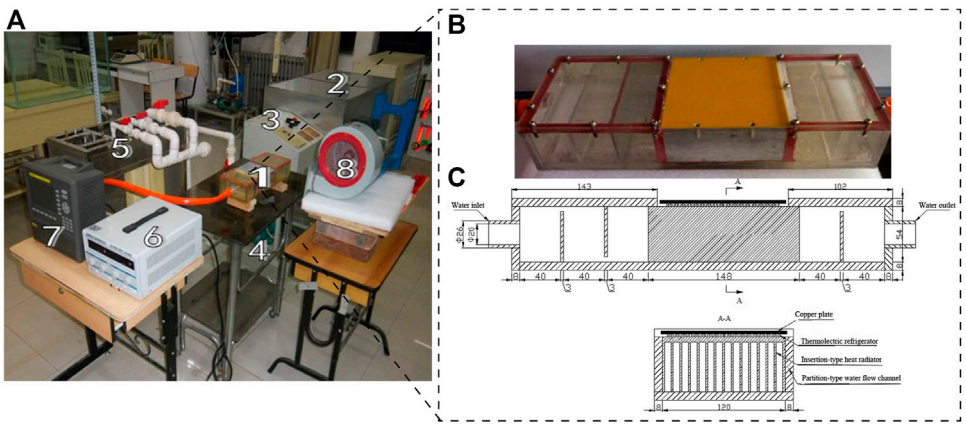


**FIGURE 2 |** Experimental system for performance research. **(A)** Experimental system platform, 1-thermoelectric refrigeration membrane distillation cold chamber, 2-water storage tank, 3-distribution box, 4-magnetic force driving circulating pump, 5-LZB type glass rotameter, 6-voltage, and current stabilization power supply, 7-TP700 multi-channel data logger, 8-fan. **(B, C)** schematic of the membrane distillation cold chamber with thermoelectric refrigeration.

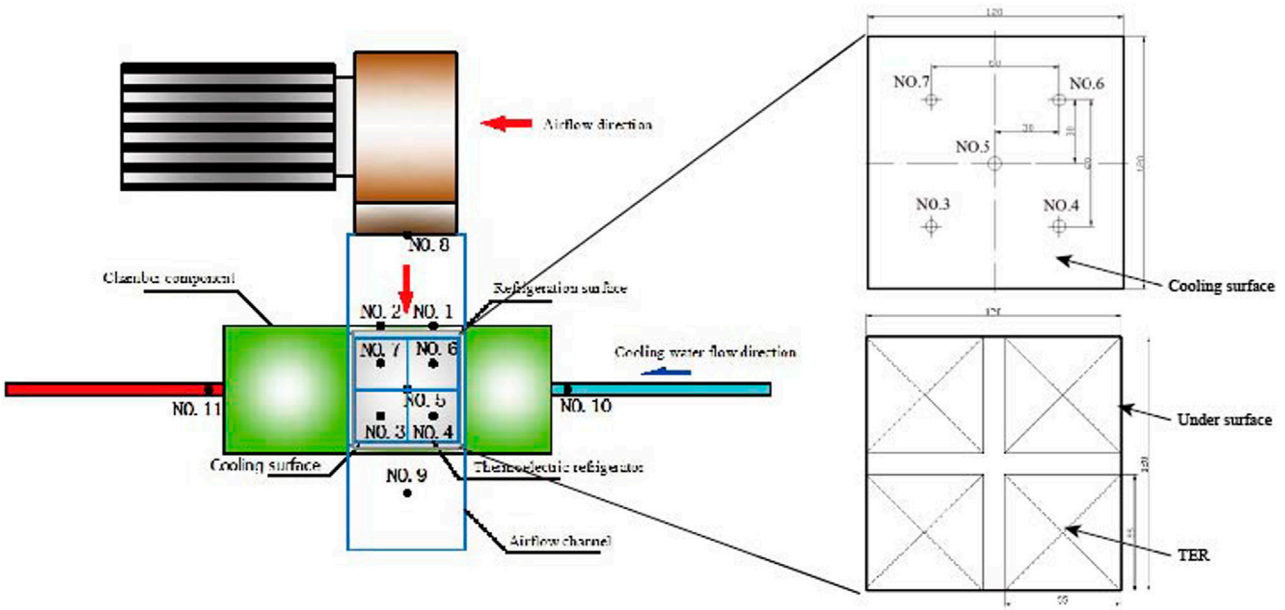


**FIGURE 3 |** Relative location of the thermocouple measurement point, unit (mm).

controlling the circulating pump to start and stop, and a frequency converter in the distribution box controls the quantity of flow of the circulating pump. Under the action of direct current, the thermoelectric refrigerator produces heat on the hot side and cooling on the cold side. In addition, heat dissipation is performed for the hot end employing water cooling, the cooling dissipation is performed for the cold end by air cooling, and the cooling dissipation is completed by a fan.

## Thermoelectric Refrigeration Membrane Distillation Cold Chamber

As shown in **Figure 2B,C**, the TERMD cold chamber mainly consists of four parts, a thermoelectric refrigerator, a heat radiator, a cold plate, and partition-type water flow channel box. A layer of thermally conductive silicone thinner than 0.02 mm is coated on both sides of the thermoelectric refrigerator, and then a copper plate is attached to the cold side. The heat radiator is placed in a position corresponding to the partition-type water flow channel box.

A 9501/242/160B type thermoelectric refrigerator with a total of four chips is selected. The dimensions of the thermoelectric refrigerator are 55 × 55 ×3.45 mm. When the thermoelectric refrigerator has a base temperature $T_h$ of 50°C, it has a maximum current of 16.0 A, a maximum voltage of 33.3 V, a maximum temperature difference $\Delta T$ of 72°C, and a maximum heat absorption amount of 289 W.

A heat exchanger of the hot side adopts an insertion-type heat radiator made of stainless steel and with dimensions of 147 × 120 ×55 mm. The dimensions of the single fin are 147 × 1.5×50.2 mm, and there are 16 fins in total. The heat exchanger of the cold end of the thermoelectric refrigerator is a copper cold plate with outer dimensions of 120 × 120 ×1.2 mm. To ensure the degree of attachment of the cold plate on the surface of the cold end of the thermoelectric refrigerator, the cold plate must own a high degree of flatness. To conveniently observe the degree of fullness of water in the channel in operation, the partition-type water flows channel box is made of organic glass.

## Experiment Produce

In the experiment, an airflow passage is adopted to drain airflow at an outlet of the fan; a four-chip thermoelectric refrigerator is in parallel connection type in the circuit and is arranged in a square. Temperature measurement points are arranged as shown in **Figure 3**, including the circulating water inlet and outlet measuring points (No. 10 and No. 11), five circulating refrigeration surface measuring points (No. 3–7), one fan outlet measuring point (No. 8), two air inlet measuring points (No. 1 and No. 2) and one air outlet measuring point (No. 9).

In the process of the experiment, the air distribution amount of the fan is 660 $m^3$/h, the circulating water temperature, and fan outlet temperature is kept stable. And the temperature signals under different working conditions are acquired by regulating the circulating water flow and working current of the thermoelectric refrigerator to obtain refrigeration capacity, to investigate the thermoelectric characteristics of the thermoelectric refrigeration membrane distillation cold chamber. To study the operational stability of the TERMD cold chamber, the experimental system is operated for 4 hours, during which the circulating water temperature, the temperature at the fan outlet, the circulating water flow, and the working current is kept stable.

## Data Measurement and Acquisition

Data measurement and acquisition consist of experiment bench parameters and temperature signal of the refrigeration surface.

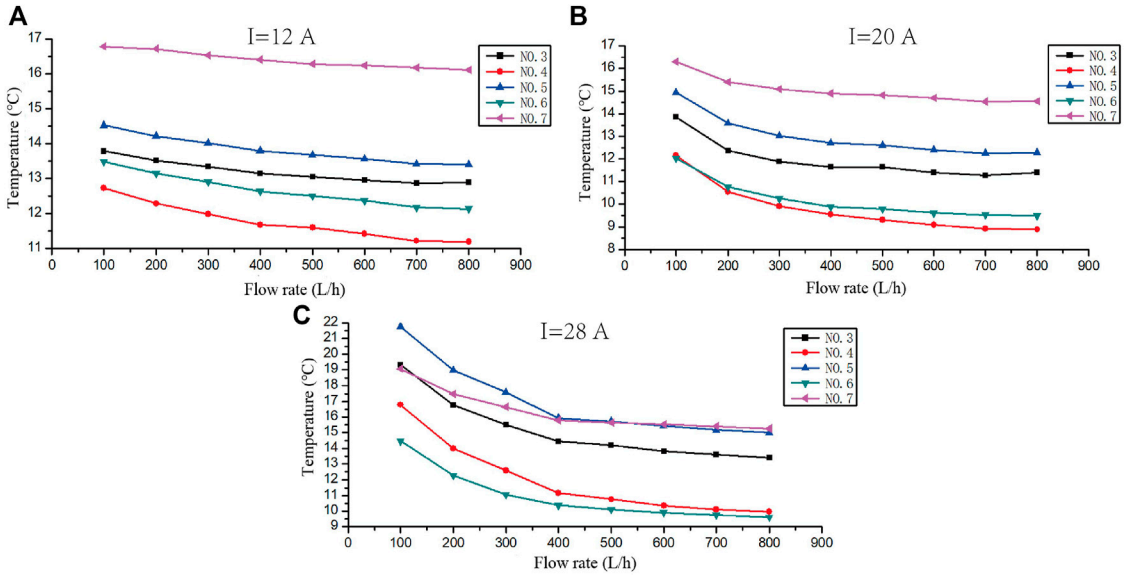


**FIGURE 4 |** Temperature variation at the ambient temperature under different circulating water flow conditions. **(A)** I = 12A, **(B)** I = 20A, and **(C)** I = 28A.

The experiment bench parameters include air distribution amount of the fan, air temperature at the outlet of the fan, circulating water flow, and temperature at the inlet and outlet of the experimental component.

The circulating water flow is metered by the glass Rotameter. The accuracy level of the glass Rotameter is 2.5, which the measurement range is (100–1,000) L/h. The stabilization power supplier is KXN-3060D, in which the measurement range is (0–30) V and (0–60) A. The PTFE membrane produced by MiL-Lipore was utilized in the air-gap membrane distillation system. The membrane pore size was 1.0 μm, the porosity was 85%, and the effective membrane area was 0.0104 $m^2$. The feed water is driven by a magnetically driven circulation pump (MP-100R-380), in which the measurement range is 7.2 $m^2$/h. The temperature is acquired by a K-type thermocouple and is automatically recorded by the TP700 multi-channel data logger. The data logger display is highly accurate, with a basic error of ± 0.2% FS. The K-type thermocouple has good linearity, large thermoelectric potential, high sensitivity, and good stability and uniformity, and the measuring range is −200–1,300°C. To ensure the accuracy of the experimental data, an experimental K-type thermocouple temperature sensor is calibrated by employing a comparison method before the experiment, a linear fitting function is adapted to perform data correction (Shengnan, 2013), and the linear fitting regression equation is highly significant at the level $\alpha = 0.01$. This experiment was carried out in Hohhot City, which is located in the Alpine region. The conclusion of the experiment is obtained in the present experimental environment and based on the precision of the equipment. The results will be more accurate if higher precision and advanced types of equipment are applied.

To ensure the reliability and accuracy of the results, the following measurement methods were employed in the explement procedures.

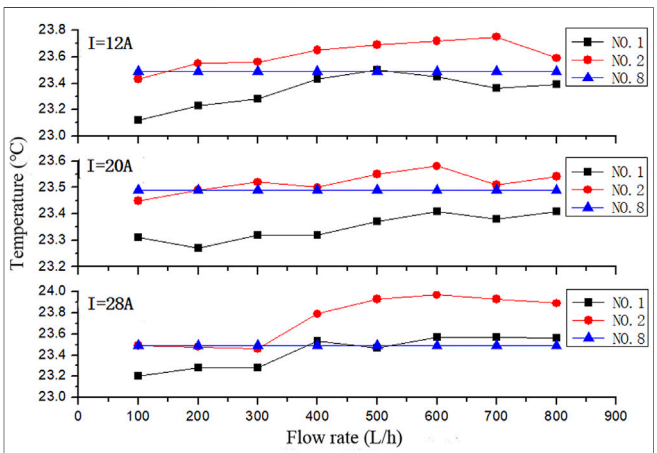


**FIGURE 5 |** Airflow temperatures at different locations.

1. All the experimental procedures were repeated three times and the obtained data were presented via the average value of the three times experiments with the errors represented by the standard deviation. The average value was calculated by dividing the sum of the values by the number of values.
2. The current to the TER was provided by a high precision constant current power source and was set to the desired value (12, 20, and 28 A).
3. Laboratory doors and windows were closed to reduce air movement during the experimental procedures. The environmental temperature of the Laboratory is about 25°C, and the humidity is around 20%.

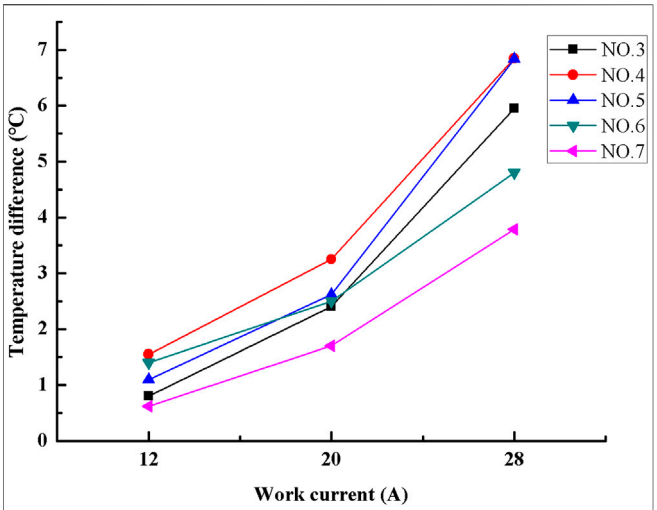


**FIGURE 6 |** Temperature differences at the measuring points under different working currents.

# RESULTS

## Influence of the Hot End Heat Dissipation Intensity on the Refrigeration Surface Temperature

Under the three current conditions I = 12 A, I = 20 A, and I = 28 A, the temperature of the refrigeration surface along with circulating cooling water flow is shown in **Figure 4**. While the input currents at I = 12 A, I = 20 A, and I = 28 A, respectively, the refrigeration surface temperature shows a decreasing tendency with the increase of the circulating cooling water flow. When the water flow volume is over 500 L/h, the temperatures of the measurement points will remain stable. It is shown that the heat dissipation intensity of the TERMD cold chamber affects the refrigeration temperature within a certain range and will not affect the refrigeration temperature after the heat dissipation intensity exceeds a maximum intensity requirement.

Both of the temperatures at measuring points No. 3 and No. 7 are greater than No. 4 and No. 6. As shown in **Figure 5**, with the fan outlet gas temperature at point No. 8, the temperature remains at 23.5°C, and the air temperatures measured at measuring point No. 2 are all higher than the No. 1. Thus, the cold end cooling dissipation intensities of the thermoelectric refrigerator corresponding to measuring points No. 3 and No. 7 are higher, thereby causing the refrigeration surface temperature to be high. That is, both of the temperatures measured at measuring points No. 3 and No. 7 are greater than the temperatures at measuring points No. 4 and No. 6.

Under different working currents, the amplitude of change of the refrigeration surface temperature is affected, while the circulating water volume flow rate increases from 100 L/h to 800 L/h. As shown in **Figure 6**, the amplitude of the change in the refrigeration surface temperature also gradually increases with the increase in the working current of the thermoelectric refrigerator. This is because of the increase in the working current, the amount of heat in the thermoelectric refrigerator gradually increases on the hot side. However, when the circulating water flow is low, the heat dissipation amount cannot be completely removed. So that part of the heat may be conducted to the refrigeration surface by the thermoelectric refrigerator, which may cause the refrigeration surface temperature to be higher.

## Influence of the Hot End Heat Dissipation Intensity on Input Power (Voltage)

When the input current maintains stability, the effects of the thermoelectric refrigerator by changing the circulating cooling water flow had been investigated as in **Figure 7**. With the increase in the circulating cooling water flow, the input voltage decreases gradually, and when the input current is I = 12 A, I = 20 A, or I = 28 A, and the water volume flow rates are greater than 200 L/h, 600 L/h, and 700 L/h, respectively, the input voltage remains constant. The input power corresponding to the water volume flow rate at a fixed value is defined as the input power threshold. As shown in **Figure 7**, when the cold side cooling dissipation intensity of the thermoelectric refrigerator is constant, the input power decreases as the hot end heat dissipation intensity of the thermoelectric refrigerator increases.

## Thermoelectric Characteristics of the Thermoelectric Refrigeration Membrane Distillation Cold Chamber

Based on the principle of thermoelectric refrigeration and combined work procedures in the experiment concluded the relationships of refrigeration power $Q_e$, heat power $Q_h$, and input power $P$ when the system is in thermal balance, in the following equation:

$$Q_h = Q_e + P \tag{1}$$

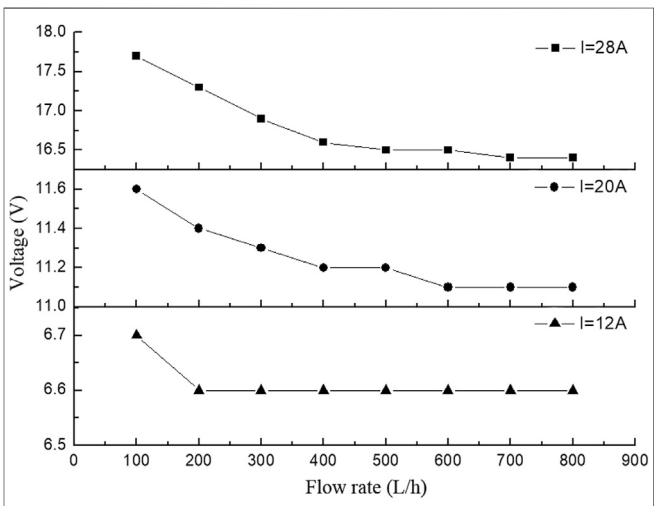


**FIGURE 7 |** Variation tendency of the working voltage with the circulating water flow rates.

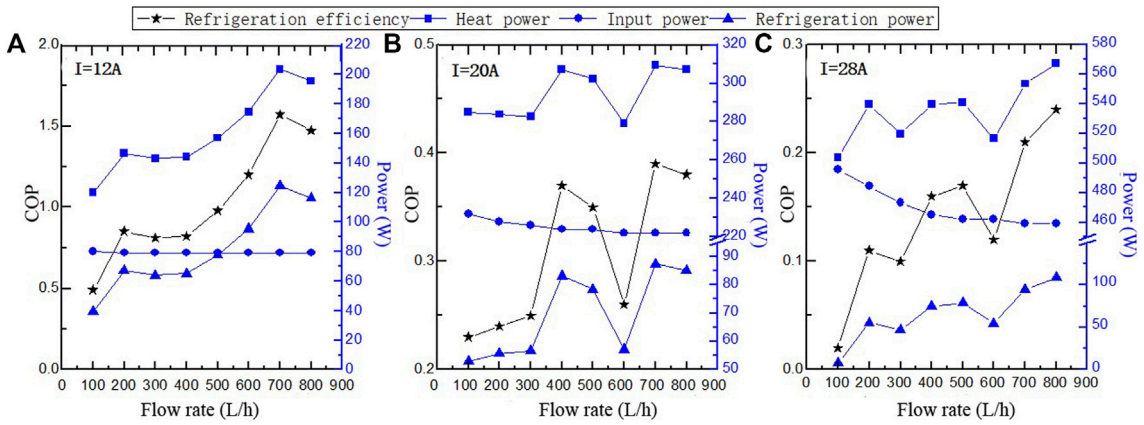


**FIGURE 8 |** Variation tendency of refrigeration performance with the increase of circulating water flow. **(A)** I = 12A, **(B)** I = 20A, and **(C)** I = 28A.

$Q_h$ is the heating capacity of the heat pump defined as (**Eq. 2**);

$$Q_h = C_P \rho Q_V \Delta T = C_P \rho Q_V \left(T_{h,in} - T_{h,out}\right) \tag{2}$$

wherein, $C_P$ denotes the specific heat capacity of the circulating cooling water, $C_P = 4.183\,(Kj/Kg \cdot k)$; $Q_V$ denotes the volume flow of the circulating cooling water, mL/s; $\rho$ denotes the density of the circulating cooling water, $\rho = 1g/ml$; $\Delta T$ denotes the difference between temperatures at the inlet ($T_{h,in}$) and the outlet ($T_{h,out}$) of the circulating cooling water, K; $U$ denotes the working voltage of the thermoelectric refrigerator, V; and $I$ denotes the working current of the thermoelectric refrigerator, A.

The Coefficient of Performance (COP) is defined as the ratio of the cooling power. (**Eq. 3**).

$$COP = \frac{Q_e}{P} = \frac{C_P \rho Q_V \Delta T - UI}{UI} \tag{3}$$

Under different working currents, the variation of the circulating cooling water flow results in the change of the COP, the heating power (increasing the thermal power consumed in a unit of time), the refrigeration power (reducing the thermal power consumed in a unit of time), and the input power, as shown in **Figure 8**. With the increase in the circulating cooling water volume flow rate, the healing power, the refrigeration power, and the input power all show an undulating rising tendency. When the input current is I = 12 A and I = 20 A, the COP, the healing power, and the refrigeration power reaches maxima of 203 W, 1.49, 123, 311 W, 0.39, and 86 W, respectively, at the water volume flow rate of 700 L/h. When the input current is I = 28 A, the COP, the healing power, and the refrigeration power reach maxima of 568 W, 0.24, and 115 W, at the water volume flow rate of 800 L/h. Thus, the refrigeration performance of the thermoelectric refrigerator can be improved by increasing the hot side heat dissipation intensity. The hot side heat dissipation intensity of the thermoelectric refrigerator can be increased by optimizing the hot side heat dissipation structure, such as, increasing the water volume flow rate of the hot side heat dissipation working medium of the thermoelectric refrigerator and decreasing the temperature of the heat dissipation working medium.

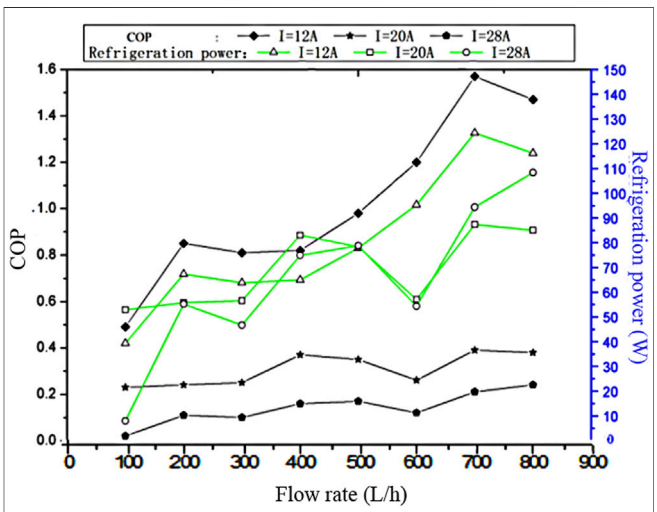


**FIGURE 9 |** Refrigeration power and COP under different working conditions.

Refrigeration power and COP are usually significant concerns when the thermoelectric refrigerator is applied to the refrigeration component. As shown in **Figure 9**, when the working current I of the thermoelectric refrigeration component is 12 A, a maximum COP is 1.57, the minimum COP is 0.49. Also, the minimum refrigeration power at the current condition 12 A is greater than the maximum COP at 20 and 28 A. Compared with the refrigeration powers of the three current conditions, the refrigeration powers are similar at flow conditions are 100 L/h and 400 L/h. However, the refrigeration power is further higher at 12 A than other input current refrigeration conditions when the flow rate is over 500 L/h. As seen from the above analysis of the thermoelectric performance, the thermoelectric refrigeration component can provide great refrigeration power and high COP under small current conditions.

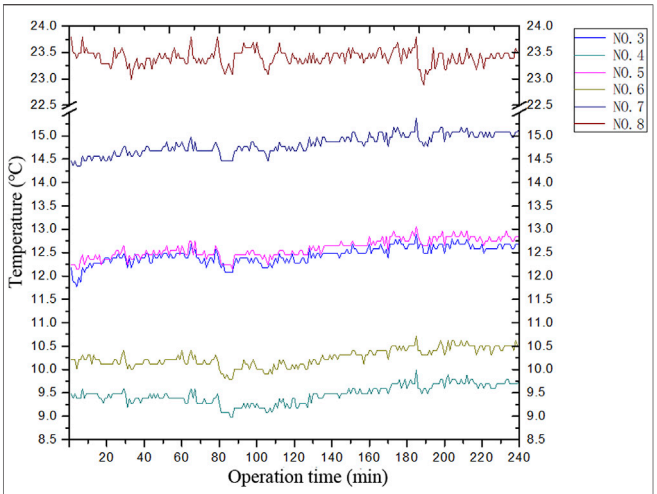


**FIGURE 10 |** Real-time temperature curves over 4 hours of continuous operation.

## Operation Stability

As shown in **Figure 10**, after the thermoelectric refrigerator operated stably for 4 hours, the temperatures are maintained at 12.5, 9.5, 12.6, 10.3, and 14.9°C approximately at No. 3–7 of the refrigeration surface. While heat dissipation intensities remain stable at both ends of the thermoelectric refrigerator, the refrigeration surface temperature can remain essentially stable for a long time. It is indicated that the performance of the thermoelectric refrigerator possesses excellent stability.

## CONCLUSION

In this paper, an experiment was performed to study the performance of the TERMDC cold chamber. Three working currents (12, 20, and 28 A) and five water flows (100–800 L/h) were considered. The performance of the TERMDC cold chamber was discussed. The conclusions are summarized as follows:

1) When the input current of the TREMD cold chamber is constant, with the increase in the heat dissipation intensity, the refrigeration temperature decreases gradually. while the water volume flow rate is over 600 L/h, the decrease tends to be stable.
2) When the cooling dissipation intensity of the TERMD cold chamber remains constant, the input power decreases as the heat dissipation intensity increases. When the water volume flow rate exceeds 500 L/h, the input power no longer decreases.
3) When the operating current of the TERMDC is 12 A, the maximum cooling efficiency is 1.57, and the minimum value is 0.49. From the analysis of the thermoelectric performance of the TERMD cold chamber, the thermoelectric refrigeration cold chamber component is capable of providing great refrigeration power and high COP under small current conditions.
4) If the heat dissipation intensities remain stable at the thermoelectric refrigerator on both sides, the performance of the TERMDC can remain constant for a long time.

## DATA AVAILABILITY STATEMENT

The original contributions presented in the study are included in the article/Supplementary Materials, further inquiries can be directed to the corresponding author.

## AUTHOR CONTRIBUTIONS

JH: Investigation, Formal Analysis, Writing Original Draft, and Reviewing. SW: Fabrication, Writing Original Draft, Methodology, and Investigation. HL: Resources and Writing's Reviewing. XY: Resources, Conceptualization, Editing, Reviewing, and Supervision.

## FUNDING

Project funding: NSFC funding project (No. 51866011).

## REFERENCES

Al-Madhhachi, H., and Min, G. (2017). Effective Use of thermal Energy at Both Hot and Cold Side of Thermoelectric Module for Developing Efficient Thermoelectric Water Distillation System. *Energ. Convers. Manage.* 133, 14–19. doi:10.1016/j.enconman.2016.11.055

Al-Madhhachi, H., and Min, G. (2018). Key Factors Affecting the Water Production in a Thermoelectric Distillation System. *Energ. Convers. Manage.* 165, 459–464. doi:10.1016/j.enconman.2018.03.080

Al-Nimr, M. d. A., and Al-Ammari, W. A. (2020). A Novel Hybrid and Interactive Solar System Consists of Stirling Engine/vacuum Evaporator/thermoelectric Cooler for Electricity Generation and Water Distillation. *Renew. Energ.* 153, 1053–1066. doi:10.1016/j.renene.2020.02.072

Alhuyi Nazari, M., Salem, M., Mahariq, I., Younes, K., and Maqableh, B. B. (2021). Utilization of Data-Driven Methods in Solar Desalination Systems: A Comprehensive Review. *Front. Energ. Res.* 9, 541. doi:10.3389/fenrg.2021.742615

Da, L., Xiaohong, Y., and Rui, T. (2019). Multi-objective Analysis and Optimization of Thermoelectric Refrigeration Membrane Distillation Experiment. *Proceedings of the CSEE* 39 (23), 10.

DuChanois, R. M., Porter, C. J., Violet, C., Verduzco, R., and Elimelech, M. (2021). Membrane Materials for Selective Ion Separations at the Water-Energy Nexus. *Adv. Mater.* 33 (38), 2101312. doi:10.1002/adma.202101312

Eslami, M., Tajeddini, F., and Etaati, N. (2018). Thermal Analysis and Optimization of a System for Water Harvesting from Humid Air Using Thermoelectric Coolers. *Energ. Convers. Manage.* 174, 417–429. doi:10.1016/j.enconman.2018.08.045

Gong, B., Yang, H., Wu, S., Xiong, G., Yan, J., Cen, K., et al. (2019). Graphene Array-Based Anti-fouling Solar Vapour Gap Membrane Distillation with High Energy Efficiency. *Nano-micro Lett.* 11 (1), 51. doi:10.1007/s40820-019-0281-1

Javadi Yanbolagh, D., Mazaheri, H., Saraei, A., and Jafari Mehrabadi, S. (2020). Experimental Study on the Performance of Three Identical Solar Stills with Different Heating Methods and External Condenser Fully Powered by Photovoltaic: Energy, Exergy, and Economic Analysis. *Energy Sourc. A: Recovery, Utilization, Environ. Effects*, 1–21. doi:10.1080/15567036.2020.1817187

Junhu, H., Xiaohong, Y., Rui, T., Kui, X., Wenlong, W., Yang, X., et al. (2015). Thermoelectric Membrane Distillation Component Energy Dissipation experiment Research. *Membr. Sci. Technol.* 35 (4), 65–71. doi:10.16159/j.cnki.issn1007-8924.2015.04.013

Junhu, H., Xiaohong, Y., and Rui, T. (2017). Study on Coupling Optimization of Thermoelectric Refrigeration and Solar Air Gap Membrane Distillation. *Journal of Solar Energy*. 38(2), 409–415.

Karahan, H. E., Goh, K., Zhang, C., Yang, E., Yıldırım, C., Chuah, C. Y., et al. (2020). MXene Materials for Designing Advanced Separation Membranes. *Adv. Mater.* 32 (29), 1906697. doi:10.1002/adma.201906697

Liao, X., Goh, K., Liao, Y., Wang, R., and Razaqpur, A. G. (2021). Bio-inspired Super Liquid-Repellent Membranes for Membrane Distillation: Mechanisms, Fabrications and Applications. *Adv. Colloid Interf. Sci.* 297, 102547. doi:10.1016/j.cis.2021.102547

Liu, G. L., Zhu, C., Cheung, C. S., and Leung, C. W. (1998). Theoretical and Experimental Studies on Air gap Membrane Distillation. *Heat Mass. Transfer* 34 (4), 329–335. doi:10.1007/s002310050267

Long, R., Li, B., Liu, Z., and Liu, W. (2016a). Ecological Analysis of a Thermally Regenerative Electrochemical Cycle. *Energy* 107, 95–102. doi:10.1016/j.energy.2016.04.004

Long, R., Li, B., Liu, Z., and Liu, W. (2016b). Performance Analysis of a Solar-Powered Electrochemical Refrigerator. *Chem. Eng. J.* 284, 325–332. doi:10.1016/j.cej.2015.09.021

Ma, Q., Xu, Z., and Wang, R. (2021). Distributed Solar Desalination by Membrane Distillation: Current Status and Future Perspectives. *Water Res.* 198, 117154. doi:10.1016/j.watres.2021.117154

Makanjuola, O., Lalia, B. S., and Hashaikeh, R. (2021). Thermoelectric Heating and Cooling for Efficient Membrane Distillation. *Case Stud. Therm. Eng.* 28, 101540. doi:10.1016/j.csite.2021.101540

Meindersma, G. W., Guijt, C. M., and de Haan, A. B. (2006). Desalination and Water Recycling by Air gap Membrane Distillation. *Desalination* 187 (1), 291–301. doi:10.1016/j.desal.2005.04.088

Min, G., Rowe, D. M., and Kontostavlakis, K. (2004). Thermoelectric Figure-Of-merit under Large Temperature Differences. *J. Phys. D: Appl. Phys.* 37 (8), 1301–1304. doi:10.1088/0022-3727/37/8/020

Nthunya, L. N., Bopape, M. F., Mahlangu, O. T., Mamba, B. B., Van der Bruggen, B., Quist-Jensen, C. A., et al. (2022). Fouling, Performance and Cost Analysis of Membrane-Based Water Desalination Technologies: A Critical Review. *J. Environ. Manage.* 301, 113922. doi:10.1016/j.jenvman.2021.113922

Parsa, S. M., Rahbar, A., Koleini, M. H., Aberoumand, S., Afrand, M., and Amidpour, M. (2020). A Renewable Energy-Driven Thermoelectric-Utilized Solar Still with External Condenser Loaded by Silver/nanofluid for Simultaneously Water Disinfection and Desalination. *Desalination* 480, 114354. doi:10.1016/j.desal.2020.114354

Pourkiaei, S. M., Ahmadi, M. H., Sadeghzadeh, M., Moosavi, S., Pourfayaz, F., Chen, L., et al. (2019). Thermoelectric Cooler and Thermoelectric Generator Devices: A Review of Present and Potential Applications, Modeling and Materials. *Energy* 186, 115849. doi:10.1016/j.energy.2019.07.179

Rahbar, N., Esfahani, J. A., and Asadi, A. (2016). An Experimental Investigation on Productivity and Performance of a New Improved Design Portable Asymmetrical Solar Still Utilizing Thermoelectric Modules. *Energ. Convers. Manage.* 118, 55–62. doi:10.1016/j.enconman.2016.03.052

Rezaei, M., Warsinger, D. M., Lienhard, V. J. H., Duke, M. C., Matsuura, T., and Samhaber, W. M. (2018). Wetting Phenomena in Membrane Distillation: Mechanisms, Reversal, and Prevention. *Water Res.* 139, 329–352. doi:10.1016/j.watres.2018.03.058

Shengnan, Y. (2013). *Application of Thermoelectric Refrigeration in Air-gap Membrane Distillation System*. Hohhot: Inner Mongolia University of Technology.

Shtull-Trauring, E., Cohen, A., Ben-Hur, M., Tanny, J., and Bernstein, N. (2020). Reducing Salinity of Treated Waste Water with Large Scale Desalination. *Water Res.* 186, 116322. doi:10.1016/j.watres.2020.116322

Smolders, K., and Franken, A. C. M. (1989). Terminology for Membrane Distillation. *Desalination* 72 (3), 249–262. doi:10.1016/0011-9164(89)80010-4

Wang, S., Shen, J., M.Santosh, M., Li, Y., Yang, C., and Ma, L. (2021). Thermoelectric Characteristics of Semiconductor Minerals in Earth's Deep Crust and Their Seismogenic Significance. *Geosci. Front.* 101337, 101337. doi:10.1016/j.gsf.2021.101337

Xh Yang, R. T., and Li, H. (2015). "Orthogonal experiment of Thermoelectric Refrigeration Membrane Distillation System," in Proceedings of china-eu membrane technology research and application seminar, weihai, shan dong, 2015, 82–86.

**Conflict of Interest:** The authors declare that the research was conducted in the absence of any commercial or financial relationships that could be construed as a potential conflict of interest.

**Publisher's Note:** All claims expressed in this article are solely those of the authors and do not necessarily represent those of their affiliated organizations, or those of the publisher, the editors and the reviewers. Any product that may be evaluated in this article, or claim that may be made by its manufacturer, is not guaranteed or endorsed by the publisher.